Vol. 8 (2015) *Acta Physica Polonica B Proceedings Supplement* No 4

MUELLER–NAVELET JETS AT THE LHC*

B. Ducloué

Department of Physics, University of Jyväskylä
P.O. Box 35, 40014, University of Jyväskylä, Finland
and
Helsinki Institute of Physics, P.O. Box 64, 00014 University of Helsinki, Finland

L. Szymanowski

National Centre for Nuclear Research (NCBJ), Warszawa, Poland

S. Wallon

Laboratoire de Physique Théorique, UMR 8627
CNRS, Univ. Paris Sud, Université Paris Saclay, 91405 Orsay, France
and
UPMC Université Paris 6, Faculté de Physique
4 place Jussieu, 75252 Paris Cedex 05, France

(Received December 7, 2015)

We report on our NLL BFKL studies of the Mueller–Navelet jets. We first perform a complete NLL BFKL analysis supplemented by a BLM renormalization scale fixing procedure, which is successfully compared with recent CMS data. Second, we argue for the need of a measurement of an asymmetric jet configuration in order to perform a valuable comparison with fixed order approaches. Third, we predict that the energy-momentum violation is rather tiny in the NLL BFKL approach, for an asymmetric jet configuration. Finally, we argue that the double parton scattering contribution is negligible in the kinematics of actual CMS measurements.

DOI:10.5506/APhysPolBSupp.8.923
PACS numbers: 12.38.Cy, 12.38.Qk, 13.85.Hd

1. Introduction

The high energy dynamics of QCD, described by the Balitsky–Fadin–Kuraev–Lipatov (BFKL) approach [1–4], have been the subject of intense studies since four decades. The production of two forward jets separated by

* Presented at EDS Blois 2015: The 16th Conference on Elastic and Diffractive Scattering, Borgo, Corsica, France, June 29–July 4, 2015.

a large interval of rapidity at hadron colliders, as proposed by Mueller and Navelet [5], is one of the most promising observables in order to reveal these dynamics. We here report on our study of this process in a next-to-leading logarithmic (NLL) BFKL approach.

The BFKL treatment involves two main building blocks, the jet vertex and Green's function. Our complete NLL BFKL analysis of Mueller–Navelet jets, including the NLL corrections both to Green's function [6,7] and to the jet vertex [8,9], demonstrated that the NLL corrections to the jet vertex have a very large effect, leading to a lower cross section and a much larger azimuthal correlation [10]. However, these findings are very dependent on the choice of the scales, especially the renormalization scale $\mu_{\rm R}$ and the factorization scale $\mu_{\rm F}$, a fact which remains true when using realistic kinematical cuts for LHC experiments [11]. In order to reduce this dependency, we then used the Brodsky, Lepage and Mackenzie (BLM) scheme [12]. The net result is that one can obtain a very satisfactory description [13] of the most recent LHC data extracted by the CMS Collaboration for the azimuthal correlations of these jets [14,15].

After a recall of these NLL results, we discuss the relevance of energy-momentum conservation in our NLL BFKL treatment. We then evaluate the importance of the potential contribution of multiparton interaction (MPI).

2. BFKL approach

The production of two jets of transverse momenta $\boldsymbol{k}_{J,1}$, $\boldsymbol{k}_{J,2}$ and rapidities $y_{J,1}$, $y_{J,2}$ is described by the differential cross section

$$\frac{d\sigma}{d|\boldsymbol{k}_{J,1}|\,d|\boldsymbol{k}_{J,2}|\,dy_{J,1}\,dy_{J,2}} = \sum_{a,b}\int_0^1 dx_1 \int_0^1 dx_2\, f_a(x_1) f_b(x_2) \times \frac{d\hat{\sigma}_{a,b}}{d|\boldsymbol{k}_{J,1}|\,d|\boldsymbol{k}_{J,2}|\,dy_{J,1}\,dy_{J,2}}\,, \tag{1}$$

where $f_{a,b}$ are the usual collinear partonic distributions (PDF). In the BFKL framework, the partonic cross section reads

$$\frac{d\hat{\sigma}_{a,b}}{d|\boldsymbol{k}_{J,1}|\,d|\boldsymbol{k}_{J,2}|\,dy_{J,1}\,dy_{J,2}} = \int d\phi_{J,1}\,d\phi_{J,2} \int d^2\boldsymbol{k}_1\,d^2\boldsymbol{k}_2\, V_a(-\boldsymbol{k}_1, x_1)\, G(\boldsymbol{k}_1, \boldsymbol{k}_2, \hat{s}), V_b(\boldsymbol{k}_2, x_2)\,, \tag{2}$$

where $V_{a,b}$ and G are respectively the jet vertices and the BFKL Green's function. One should note that the use of conventional PDF in Eq. (1) is justified by the fact that the rapidity $Y = y_{J,1} - y_{J,2}$ is large enough so that

the momentum fractions x_1 and x_2 are not parametrically small. Besides the cross section, the azimuthal correlation of the two jets is another relevant observable sensitive to resummation effects [16, 17]. Denoting as $\phi_{J,1}$, $\phi_{J,2}$ the azimuthal angles of the two jets, and defining the relative azimuthal angle φ such that $\varphi = 0$ corresponds to the back-to-back configuration, the moments of this distribution read

$$\langle \cos(n\varphi) \rangle \equiv \langle \cos\left(n\left(\phi_{J,1} - \phi_{J,2} - \pi\right)\right) \rangle = \frac{\mathcal{C}_n}{\mathcal{C}_0}\,, \tag{3}$$

with

$$\mathcal{C}_0 = \frac{d\sigma}{d|\boldsymbol{k}_{J,1}|\, d|\boldsymbol{k}_{J,2}|\, dy_{J,1}\, dy_{J,2}} \tag{4}$$

and

$$\mathcal{C}_n = (4 - 3\delta_{n,0}) \int d\nu\, C_{n,\nu}\left(|\boldsymbol{k}_{J,1}|, x_{J,1}\right) C^*_{n,\nu}\left(|\boldsymbol{k}_{J,2}|, x_{J,2}\right) \left(\frac{\hat{s}}{s_0}\right)^{\omega(n,\nu)}\,. \tag{5}$$

The coefficients $C_{n,\nu}$ are given by

$$C_{n,\nu}(|\boldsymbol{k}_J|, x_J) = \int d\phi_J\, d^2\boldsymbol{k}\, dx\, f(x) V(\boldsymbol{k}, x) E_{n,\nu}(\boldsymbol{k}) \cos(n\phi_J)\,, \tag{6}$$

where

$$E_{n,\nu}(\boldsymbol{k}) = \frac{1}{\pi\sqrt{2}} \left(\boldsymbol{k}^2\right)^{i\nu - \frac{1}{2}} e^{in\phi}\,. \tag{7}$$

At leading logarithmic (LL) accuracy, the jet vertex reads

$$V_a(\boldsymbol{k}, x) = V_a^{(0)}(\boldsymbol{k}, x) = \frac{\alpha_{\rm s}}{\sqrt{2}} \frac{C_{A/F}}{\boldsymbol{k}^2} \delta\left(1 - \frac{x_J}{x}\right) |\boldsymbol{k}_J| \delta^{(2)}(\boldsymbol{k} - \boldsymbol{k}_J)\,, \tag{8}$$

with $C_A = N_{\rm c} = 3$ (incoming gluon) and $C_F = (N_{\rm c}^2 - 1)/(2N_{\rm c}) = 4/3$ (incoming quark). The expressions of the next-to-leading order (NLO) corrections to V_a [8, 9, 18–20] can be found in Ref. [10]. They have been computed in the limit of small cone jets in Ref. [21] and used in Refs. [22–26] (see also [27]). The LL BFKL trajectory reads

$$\omega(n, \nu) = \bar{\alpha}_{\rm s} s \left[2\Psi(1) - \Psi\left(\frac{n+1}{2} + i\nu\right) - \Psi\left(\frac{n+1}{2} - i\nu\right)\right]\,, \tag{9}$$

where $\bar{\alpha}_{\rm s} s = N_{\rm c}\alpha_{\rm s}/\pi$, while at NLL, its analytical expression is much more involved [28–33], see Ref. [11] for explicit formulas.

Even at NLL accuracy, several observables depend strongly on the choice of the scales, and, in particular, the renormalization scale $\mu_{\rm R}$. An optimization procedure to fix the renormalization scale allows to reduce this dependency. We use the BLM procedure [12], which is a way of absorbing the

non-conformal terms of the perturbative series in a redefinition of the coupling constant, to improve the convergence of the perturbative series. The first practical implementation of the BLM procedure in the context of BFKL was performed in Refs. [34–37]. In Refs. [36, 37], it was argued that, when dealing with BFKL calculations, the BLM procedure is more conveniently applied in a physical renormalization scheme like the MOM scheme instead of the usual $\overline{\text{MS}}$ scheme, a method followed in Refs. [38–40]. The observables introduced above in the $\overline{\text{MS}}$ scheme can be obtained in the MOM scheme using [41, 42]

$$\alpha_{\overline{\text{MS}}} = \alpha_{\text{MOM}} \left(1 + \alpha_{\text{MOM}} \frac{T_{\text{MOM}}}{\pi} \right) , \tag{10}$$

where

$$\begin{aligned} T_{\text{MOM}} &= T^{\beta}_{\text{MOM}} + T^{\text{conf}}_{\text{MOM}} , \\ T^{\text{conf}}_{\text{MOM}} &= \frac{N_c}{8} \left[\frac{17}{2} I + \frac{3}{2} (I-1)\, \xi + \left(1 - \frac{1}{3} I \right) \xi^2 - \frac{1}{6} \xi^3 \right] , \\ T^{\beta}_{\text{MOM}} &= -\frac{\beta_0}{2} \left(1 + \frac{2}{3} I \right) , \end{aligned} \tag{11}$$

where $I = -2 \int_0^1 dx \ln(x)/[x^2 - x + 1] \simeq 2.3439$ and ξ is the covariant gauges parameter. Performing the transition from the $\overline{\text{MS}}$ to the MOM schemes, one should then choose the renormalization scale to make the β_0-dependent part vanish. This is achieved with

$$\mu^2_{\text{R,BLM}} = |\boldsymbol{k}_{J,1}| \cdot |\boldsymbol{k}_{J,2}| \exp \left[\tfrac{1}{2} \chi_0(n,\gamma) - \tfrac{5}{3} + 2 \left(1 + \tfrac{2}{3} I \right) \right] . \tag{12}$$

3. Results: symmetric and asymmetric configurations

3.1. Symmetric configuration and CMS data

We first compare our results with the measurement performed by the CMS Collaboration on the azimuthal correlations of Mueller–Navelet jets at the LHC at a center-of-mass energy $\sqrt{s} = 7$ TeV [14]. The two jets have transverse momenta larger than 35 GeV and rapidities lower than 4.7. We use the anti-k_t jet algorithm [43] with a size parameter $R = 0.5$ and the MSTW 2008 [44] parametrization for the PDFs. In the plots of Figs. 1 and 2, we show the CMS data (black dots with error bars), the NLL BFKL result using the "natural" scale choice $\mu_{\text{R}} = \sqrt{|\boldsymbol{k}_{J,1}| \cdot |\boldsymbol{k}_{J,2}|}$ (solid black line) and the NLL BFKL results using the BLM scale setting (gray error band[1]).

[1] The gray error band corresponds to the typical theoretical uncertainty when practically implementing the BLM procedure.

Our results for the angular correlations $\langle \cos \varphi \rangle$ and $\langle \cos 2\varphi \rangle$ as a function of Y are shown in Fig. 1 (left) and (right) respectively. For these two observables, the NLL BFKL calculation with the "natural" scale choice predicts a strong correlation, while using the BLM procedure to fix the renormalization scale leads to a very good agreement with the data.

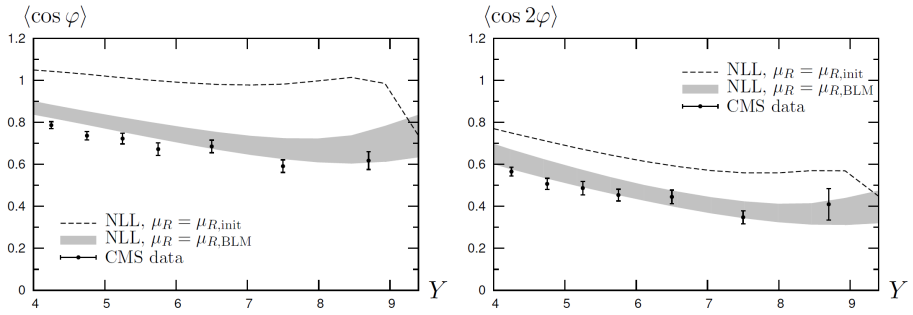

Fig. 1. Symmetric configuration. Left: Variation of $\langle \cos \varphi \rangle$ as a function of Y at NLL accuracy compared with CMS data. Right: Variation of $\langle \cos 2\varphi \rangle$ as a function of Y at NLL accuracy compared with CMS data.

This improvement due to the BLM procedure is most clearly seen through the azimuthal distribution of the jets $\frac{1}{\sigma}\frac{d\sigma}{d\varphi}$

$$\frac{1}{\sigma}\frac{d\sigma}{d\varphi} = \frac{1}{2\pi}\left\{1 + 2\sum_{n=1}^{\infty} \cos(n\varphi)\,\langle \cos(n\varphi)\rangle\right\}, \tag{13}$$

as displayed in Fig. 2 (left).

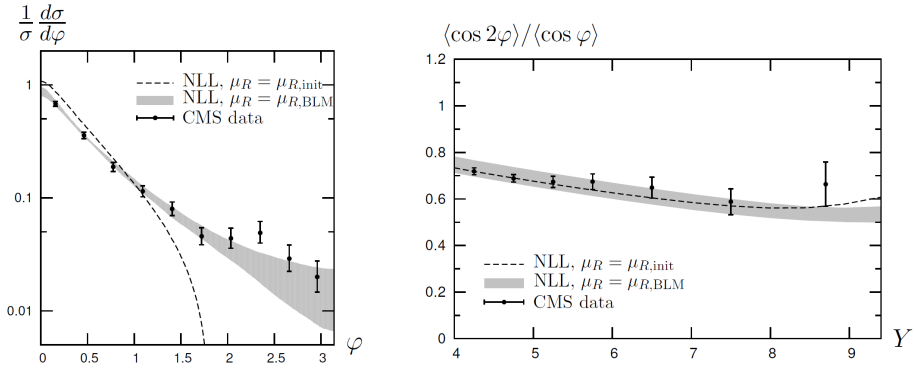

Fig. 2. Symmetric configuration. Left: Azimuthal distribution at NLL accuracy compared with CMS data. Right: Variation of $\langle \cos 2\varphi \rangle / \langle \cos \varphi \rangle$ as a function of Y at NLL accuracy compared with CMS data.

It was already observed both at LL and NLL accuracy [10, 11, 31–33] that ratios of the kind $\langle \cos m\varphi \rangle / \langle \cos n\varphi \rangle$ with $n \neq 0$ are much more stable with respect to the scales than individual moments $\langle \cos n\varphi \rangle$ and, therefore, are almost not affected by the BLM procedure. Indeed, Fig. 2 (right) for $\langle \cos 2\varphi \rangle / \langle \cos \varphi \rangle$ shows that the good agreement with the data was obtained when using either the "natural" scale or the BLM procedure.

3.2. Asymmetric configuration: BFKL versus fixed order

It is well-known that fixed-order calculations are unstable when the lower cut on the transverse momenta of both jets is the same [45, 46]. This is the situation encountered by the above CMS measurement [14]. Still, a comparison of the agreement of a fixed-order calculation and of a BFKL one with data would be very useful to further investigate the need for resummation effects at high energy. We now choose the lower cut on the transverse momenta of the jets to slightly differ. In practice, this is implemented by taking the same cuts as above, but now with the additional requirement that the transverse momentum of at least one jet is larger than 50 GeV, making the fixed-order calculation now trustable. As discussed previously, the quantities $\langle \cos n\varphi \rangle$ are not very stable even at NLL accuracy in the BFKL approach, so that a comparison with a fixed-order calculation for these observables would not be very meaningful. On the contrary, the observable $\langle \cos 2\varphi \rangle / \langle \cos \varphi \rangle$ is more stable in the BFKL approach. Figure 3 shows the comparison of the NLL BFKL calculation with the results obtained with the NLO fixed-order code Dijet [47] and clearly demonstrates that a sizable difference between the two treatments is expected over a large Y range.

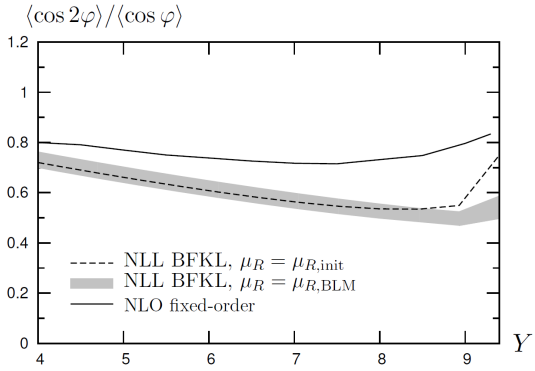

Fig. 3. Asymmetric configuration. Variation of $\langle \cos 2\varphi \rangle / \langle \cos \varphi \rangle$ as a function of Y at NLL accuracy compared with a fixed-order treatment.

One should note that in the very peculiar situation where the two jets are almost back-to-back, for which a fixed-order calculation is unstable, resummation effects *à la* Sudakov should be considered to stabilize the calculation. In the BFKL approach, although this back-to-back limit is stable, the azimuthal distribution can be significantly affected by such resummation effects. These have been obtained recently in the LL approximation [48].

4. Energy-momentum conservation

It is well-known that energy-momentum conservation is not satisfied in the BFKL approach, being formally a sub-leading effect. Still, it could be numerically important, at least at LL accuracy. It was proposed [49] to evaluate the importance of this effect by comparing the results of an exact $\mathcal{O}(\alpha_s^3)$ calculation with the BFKL result, expanded in powers of α_s and truncated to the order of α_s^3. This showed that an LL BFKL calculation strongly overestimates the cross section with respect to an exact calculation as long as the two jets transverse momenta are not very similar (which is the case in the asymmetric configuration discussed above). In the same spirit, a study with LO vertices and NLL Green's function was performed in Ref. [50]. Having in mind that adding corrections beyond the LL approximation should reduce the violation of energy-momentum conservation, we here also include NLO corrections to the jet vertices [51]. Consider the effective rapidity Y_{eff} [49]

$$Y_{\text{eff}} \equiv Y \frac{\mathcal{C}_m^{2\to 3}}{\mathcal{C}_m^{\text{BFKL},\mathcal{O}(\alpha_s^3)}}, \tag{14}$$

where $\mathcal{C}_m^{2\to 3}$ is the exact $\mathcal{O}(\alpha_s^3)$ result obtained by studying the reaction $gg \to ggg$, while $\mathcal{C}_m^{\text{BFKL},\mathcal{O}(\alpha_s^3)}$ is the BFKL result expanded in powers of α_s and truncated to the order $\mathcal{O}(\alpha_s^3)$. This effective rapidity (14) has the property that if one replaces Y by Y_{eff} in the BFKL calculation, expands in powers of α_s and truncates to the order of α_s^3, the exact result is recovered. The value of Y_{eff} indicates how valid the BFKL approximation is: a value close to Y means that this approximation is valid, whereas a value significantly different from Y means that it is a too strong assumption in the kinematics under study. In Fig. 4, we show the values obtained for Y_{eff} as a function of $\boldsymbol{k}_{J,2}$ for fixed $\boldsymbol{k}_{J,1} = 35$ GeV at a center-of-mass energy $\sqrt{s} = 7$ TeV and for a rapidity separation $Y = 8$, in the LL and NLL approximation. As found in Ref. [49], the LL calculation strongly overestimates the cross section for transverse momenta of the jets not too close. At NLL accuracy, the situation is much improved for significantly different jet transverse momenta (as needed to obtain trustable results in the fixed order approach): the effective rapidity is very close to Y so that the violation of energy-momentum should be much less severe at NLL accuracy.

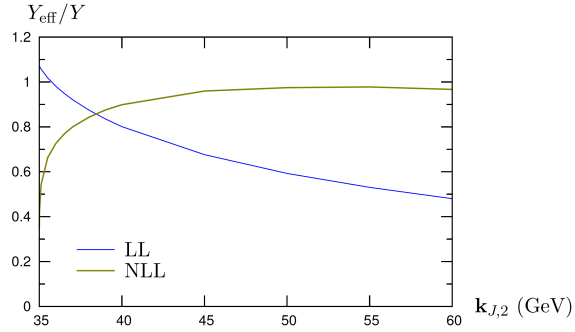

Fig. 4. Variation of $Y_{\rm eff}/Y$ as defined in Eq. (14) as a function of $\boldsymbol{k}_{J,2}$ at fixed $\boldsymbol{k}_{J,1} = 35$ GeV for $Y = 8$ and $\sqrt{s} = 7$ TeV at leading logarithmic (black/blue) and next-to-leading logarithmic (gray/brown) accuracy.

5. Double parton scattering contribution to MN jets

At high energies and low transverse momenta, where BFKL effects are expected to be enhanced, parton densities can become large enough that contributions where several partons from the same incoming hadron take part in the interaction could become important. We restrict ourselves to the case of double parton scattering where there are at most two scattering subprocesses and where both these scatterings are hard, as illustrated in Fig. 5.

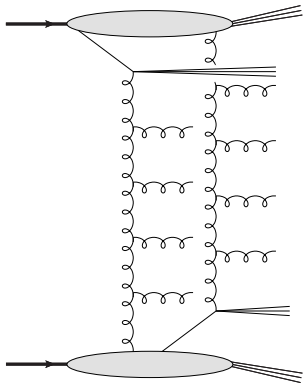

Fig. 5. The DPS contribution.

For simplicity, the order of magnitude of this contribution is evaluated at LL, which we compare with our prediction involving single parton scattering in the BFKL LL and NLL approaches. We use a simple factorized Ansatz to compute the DPS contribution according to

$$\sigma_{\rm DPS} = \frac{\sigma_{\rm fwd}\sigma_{\rm bwd}}{\sigma_{\rm eff}}\,, \tag{15}$$

where $\sigma_{\mathrm{fwd(bwd)}}$ is the inclusive cross section for one jet in the forward (backward) direction and σ_{eff} is a phenomenological quantity related to the density of the proton in the transverse plane. We vary σ_{eff} between 10 and 20 mb, to be consistent with the measurements at the Tevatron [52–55] and at the LHC [56, 57]. Each of the inclusive cross sections for one jet in the forward (backward) direction is built as the convolution of the LO jet vertex with unintegrated gluon distributions (UGD) [58–65], the global normalization being fitted with CMS [66] data (see Ref. [67] for more details), for four different parametrizations. We focus on four choices of kinematical cuts:

$$\sqrt{s} = 7 \text{ TeV}, \qquad |\boldsymbol{k}_{J,1}| = |\boldsymbol{k}_{J,2}| = 35 \text{ GeV},$$
$$\sqrt{s} = 14 \text{ TeV}, \qquad |\boldsymbol{k}_{J,1}| = |\boldsymbol{k}_{J,2}| = 35 \text{ GeV},$$
$$\sqrt{s} = 14 \text{ TeV}, \qquad |\boldsymbol{k}_{J,1}| = |\boldsymbol{k}_{J,2}| = 20 \text{ GeV},$$
$$\sqrt{s} = 14 \text{ TeV}, \qquad |\boldsymbol{k}_{J,1}| = |\boldsymbol{k}_{J,2}| = 10 \text{ GeV}.$$

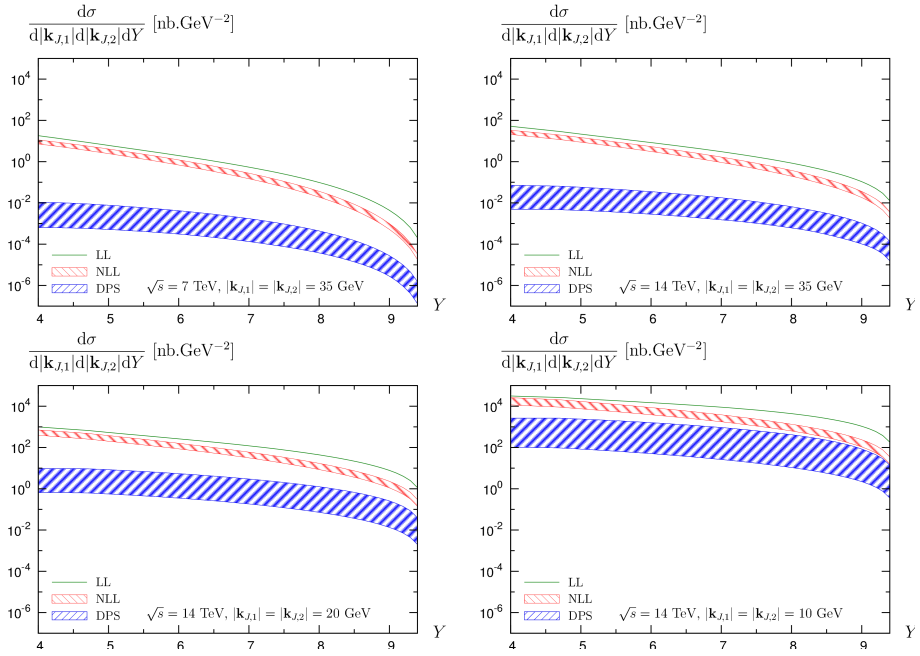

Fig. 6. Comparison of the differential cross section obtained at LL (thin solid green line) and NLL (gray/red hatched band) accuracy in the BFKL approach and the DPS cross section (black/blue hatched band) for the four kinematical cuts described in the text.

The first choice is similar to the cuts used by the CMS analysis of azimuthal correlations of Mueller–Navelet jets at the LHC [14], as displayed in Figs. 1 and 2. The other three choices correspond to the higher center-of-mass energy that the LHC is expected to reach soon. The last two choices correspond to lower transverse momenta at which measurements could become possible in the future, and are particularly relevant since MPI are expected to become more and more important at lower transverse momenta. The rapidities of the jets are restricted according to $0 < y_{J,1} < 4.7$ and $-4.7 < y_{J,2} < 0$. We use the MSTW 2008 parametrization [44] for collinear parton densities. To estimate the uncertainty associated with the choice of the UGD parametrization needed to compute the DPS cross section, we use the same four parametrizations. Our results are displayed in Fig. 6. The resulting uncertainty on the DPS cross section is rather large. Still, this cross section is always smaller than the SPS one in the LHC kinematics we considered here. The same conclusion can be addressed for the impact of double parton scattering on the angular correlation between the jets. It is only for the set of parameters giving the largest DPS contribution, *i.e.* at low transverse momenta and large rapidity separations, that the effect of DPS can become larger than the uncertainty on the NLL BFKL calculation.

6. Conclusions

The azimuthal correlations of Mueller–Navelet jets recently extracted by the CMS Collaboration can be well described by a full NLL BFKL calculation supplemented by the use of the BLM procedure to fix the renormalization scale. We also studied two effects which are claimed to have a potentially significant impact in this picture. First, we have shown that the effect of the absence of strict energy-momentum conservation in a BFKL calculation is expected to be tiny at NLL accuracy for significantly different values of transverse momenta of the tagged jets. Second, we have shown that the order of magnitude of DPS contributions is presumably negligible for the kinematics which is under consideration at the LHC. Further studies would be required at low transverse momenta and very high center-of-mass energies.

B. Ducloué acknowledges support from the Academy of Finland, Project No. 273464. This work was done using computing resources from CSC — IT Center for Science in Espoo, Finland. L. Szymanowski was partially supported by a French Government Scholarship. This work is partially supported by the French Grant ANR PARTONS No. ANR-12-MONU-0008-01.

REFERENCES

[1] V.S. Fadin, E.A. Kuraev, L.N. Lipatov, *Phys. Lett. B* **60**, 50 (1975).
[2] E.A. Kuraev, L.N. Lipatov, V.S. Fadin, *Sov. Phys. JETP* **44**, 443 (1976).
[3] E.A. Kuraev, L.N. Lipatov, V.S. Fadin, *Sov. Phys. JETP* **45**, 199 (1977).
[4] I. Balitsky, L.N. Lipatov, *Sov. J. Nucl. Phys.* **28**, 822 (1978).
[5] A.H. Mueller, H. Navelet, *Nucl. Phys. B* **282**, 727 (1987).
[6] V.S. Fadin, L.N. Lipatov, *Phys. Lett. B* **429**, 127 (1998).
[7] M. Ciafaloni, G. Camici, *Phys. Lett. B* **430**, 349 (1998).
[8] J. Bartels, D. Colferai, G.P. Vacca, *Eur. Phys. J. C* **24**, 83 (2002).
[9] J. Bartels, D. Colferai, G.P. Vacca, *Eur. Phys. J. C* **29**, 235 (2003).
[10] D. Colferai, F. Schwennsen, L. Szymanowski, S. Wallon, *J. High Energy Phys.* **1012**, 026 (2010).
[11] B. Ducloué, L. Szymanowski, S. Wallon, *J. High Energy Phys.* **1305**, 096 (2013).
[12] S.J. Brodsky, G.P. Lepage, P.B. Mackenzie, *Phys. Rev. D* **28**, 228 (1983).
[13] B. Ducloué, L. Szymanowski, S. Wallon, *Phys. Rev. Lett.* **112**, 082003 (2014).
[14] CMS Collaboration, CMS PAS FSQ-12-002, 2013.
[15] G. Safronov, "Multi-jet Measurements at CMS", talk at MPI@LHC 2015, ICTP Trieste, November 23–27, 2015.
[16] V. Del Duca, C.R. Schmidt, *Phys. Rev. D* **49**, 4510 (1994).
[17] W.J. Stirling, *Nucl. Phys. B* **423**, 56 (1994).
[18] F. Caporale *et al.*, *J. High Energy Phys.* **1202**, 101 (2012).
[19] M. Hentschinski, A. Sabio Vera, *Phys. Rev. D* **85**, 056006 (2012).
[20] G. Chachamis, M. Hentschinski, J.D. Madrigal Martínez, A. Sabio Vera, *Phys. Rev. D* **87**, 076009 (2013).
[21] D.Yu. Ivanov, A. Papa, *J. High Energy Phys.* **1205**, 086 (2012).
[22] F. Caporale, D.Yu. Ivanov, B. Murdaca, A. Papa, *Nucl. Phys. B* **877**, 73 (2013).
[23] F. Caporale, B. Murdaca, A. Sabio Vera, C. Salas, *Nucl. Phys. B* **875**, 134 (2013).
[24] F. Caporale, D.Yu. Ivanov, B. Murdaca, A. Papa, *Eur. Phys. J. C* **74**, 3084 (2014).
[25] F. Caporale, D.Yu. Ivanov, B. Murdaca, A. Papa, *Phys. Rev. D* **91**, 114009 (2015).
[26] F.G. Celiberto, D.Yu. Ivanov, B. Murdaca, A. Papa, *Eur. Phys. J. C* **75**, 292 (2015).
[27] D. Colferai, A. Niccoli, *J. High Energy Phys.* **1504**, 071 (2015).
[28] A.V. Kotikov, L.N. Lipatov, *Nucl. Phys. B* **582**, 19 (2000).
[29] A.V. Kotikov, L.N. Lipatov, *Nucl. Phys. B* **661**, 19 (2003) [*Erratum ibid.* **685**, 405 (2004)].
[30] D.Yu. Ivanov, A. Papa, *Nucl. Phys. B* **732**, 183 (2006).

[31] A. Sabio Vera, *Nucl. Phys. B* **746**, 1 (2006).
[32] A. Sabio Vera, F. Schwennsen, *Nucl. Phys. B* **776**, 170 (2007).
[33] F. Schwennsen, arXiv:hep-ph/0703198.
[34] S.J. Brodsky, F. Hautmann, D.E. Soper, *Phys. Rev. Lett.* **78**, 803 (1997) [*Erratum ibid.* **79**, 3544 (1997)].
[35] S.J. Brodsky, F. Hautmann, D.E. Soper, *Phys. Rev. D* **56**, 6957 (1997).
[36] S.J. Brodsky *et al.*, *JETP Lett.* **70**, 155 (1999).
[37] S.J. Brodsky *et al.*, *JETP Lett.* **76**, 249 (2002).
[38] M. Angioni, G. Chachamis, J.D. Madrigal, A. Sabio Vera, *Phys. Rev. Lett.* **107**, 191601 (2011).
[39] M. Hentschinski, A. Sabio Vera, C. Salas, *Phys. Rev. Lett.* **110**, 041601 (2013).
[40] M. Hentschinski, A. Sabio Vera, C. Salas, *Phys. Rev. D* **87**, 076005 (2013).
[41] W. Celmaster, R.J. Gonsalves, *Phys. Rev. Lett.* **42**, 1435 (1979).
[42] W. Celmaster, R.J. Gonsalves, *Phys. Rev. D* **20**, 1420 (1979).
[43] M. Cacciari, G.P. Salam, G. Soyez, *J. High Energy Phys.* **0804**, 063 (2008).
[44] A.D. Martin, W. Stirling, R. Thorne, G. Watt, *Eur. Phys. J. C* **63**, 189 (2009).
[45] J.R. Andersen *et al.*, *J. High Energy Phys.* **0102**, 007 (2001).
[46] M. Fontannaz, J.P. Guillet, G. Heinrich, *Eur. Phys. J. C* **22**, 303 (2001).
[47] P. Aurenche, R. Basu, M. Fontannaz, *Eur. Phys. J. C* **57**, 681 (2008).
[48] A.H. Mueller *et al.*, in preparation.
[49] V. Del Duca, C.R. Schmidt, *Phys. Rev. D* **51**, 2150 (1995).
[50] C. Marquet, C. Royon, *Phys. Rev. D* **79**, 034028 (2009).
[51] B. Ducloué, L. Szymanowski, S. Wallon, *Phys. Lett. B* **738**, 311 (2014).
[52] CDF Collaboration, *Phys. Rev. D* **47**, 4857 (1993).
[53] CDF Collaboration, *Phys. Rev. D* **56**, 3811 (1997).
[54] D0 Collaboration, *Phys. Rev. D* **81**, 052012 (2010).
[55] D0 Collabration, *Phys. Rev. D* **89**, 072006 (2014).
[56] ATLAS Collaboration, *New J. Phys.* **15**, 033038 (2013).
[57] CMS Collaboration, *J. High Energy Phys.* **1403**, 032 (2014).
[58] J. Kwiecinski, A.D. Martin, A.M. Stasto, *Phys. Rev. D* **56**, 3991 (1997).
[59] K. Golec-Biernat, M. Wusthoff, *Phys. Rev. D* **60**, 114023 (1999).
[60] M.A. Kimber, A.D. Martin, M.G. Ryskin, *Phys. Rev. D* **63**, 114027 (2001).
[61] M. Hansson, H. Jung, arXiv:hep-ph/0309009.
[62] K. Kutak, A.M. Stasto, *Eur. Phys. J. C* **41**, 343 (2005).
[63] H. Jung, arXiv:hep-ph/0411287.
[64] K. Kutak, S. Sapeta, *Phys. Rev. D* **86**, 094043 (2012).
[65] F. Hautmann, H. Jung, *Nucl. Phys. B* **883**, 1 (2014).
[66] CMS Collaboration, *J. High Energy Phys.* **1206**, 036 (2012).
[67] B. Ducloué, L. Szymanowski, S. Wallon, *Phys. Rev. D* **92**, 076002 (2015).